



# Neutron- and X-ray radiography/ tomography: non-destructive analytical tools for the characterization of nuclear materials

by F.C. de Beer\*†

## Synopsis

A number of important areas in nuclear fuel cycle, at both the front end and back end, offer ideal opportunities for the application of non-destructive evaluation techniques. These techniques do not only provide opportunities for non-invasive testing of *e.g.* irradiated materials, but also play an important role in the development of new materials in the nuclear sector. The advantage of penetrating radiation used as probe in the investigation and testing of nuclear materials makes X-ray and neutron radiography (2D) and tomography (3D) suitable for various applications in the total nuclear fuel cycle. The unique and different interaction modes of the two radiation probes with materials provide several opportunities. Their complementary nature and non-destructive character makes them most suitable for nuclear material analyses, analytical method development, and the evaluation of the performance of existing nuclear material compositions. This article gives an overview of the X-ray and neutron radiography/tomography applications in the field of nuclear material testing, and highlights a few of the success stories. Several selected areas of application in the nuclear fuel cycle are discussed to illustrate the complementary nature of these techniques as applied to nuclear materials.

## Keywords

neutron radiography, X-ray radiography, SAFARI-1; non-destructive testing.

## Introduction

During the development of new materials for the nuclear industry, materials testing and characterization are of the outmost importance to maintain safety standards and reliability. No compromise on safety in the workplace in any area within the total nuclear fuel cycle can be tolerated, and therefore most *in-situ* material characterization and testing is conducted by certified and qualified personnel schooled in destructive and non-destructive testing (DT and NDT) methods. Certification and qualification in NDT can be obtained through many training centres in South Africa in accordance with European, American, and other international standards (SGS, n.d.; SAIW, n.d.; African NTD Centre, n.d.).

The testing of new methods and materials related to the nuclear fuel cycle is essential for the continuing development and safety of nuclear-related materials and processes. These fundamental research initiatives are mostly performed at the laboratory scale by material and instrument scientists, researchers, and most likely postgraduate students.

Davies (2000) describes the role and value of NDT during maintenance and in-service inspection of nuclear power plants during outages, and particularly the monitoring of material degradation to prevent failure. Ultrasonic testing (UT), magnetic testing (MT), and electrical testing (ET) play a major role as NDT methods for monitoring materials degradation *in-situ*, while atomic- and nuclear physics-based methods such as positron annihilation, neutron diffraction, as well as X-ray and neutron tomography are limited to laboratory-scale experimentation. However, conventional film-based X-ray and gamma-ray radiography (RT) techniques are being applied throughout many areas of material testing in the nuclear fuel cycle.

The 'nuclear fuel cycle' refers to the entire range of activities associated with the production of electricity from nuclear fission, entailing (International Atomic Energy Agency, n.d.):

- Mining and milling: from mined uranium to yellowcake
- Conversion: from yellowcake to gas
- Enrichment: increases the proportion of the fissile Isotope
- Deconversion: depleted uranium.
- Fuel fabrication: UO<sub>2</sub> pellets – fuel pins – fuel elements
- Electricity generation: fuel burn-up
- Storage: spent fuel
- Reprocessing: spent fuel
- Radioactive waste: safe storage.

The nuclear fuel cycle includes the 'front end', *i.e.* preparation of the fuel, the 'service period' in which fuel is used in the reactor to generate electricity, and the 'back end', *i.e.* the safe management of spent fuel, including reprocessing and reuse and disposal.

\* Radiation Science Department, Necsa, Pelindaba.

† School of Chemical and Minerals Engineering, North-West University, Potchefstroom.

© The Southern African Institute of Mining and Metallurgy, 2015. ISSN 2225-6253. Paper received Aug. 2015 and revised paper received Aug. 2015.

## Neutron- and X-ray radiography/tomography

The general nuclear fuel cycle is schematically depicted in Figure 1, showing the various activities in the production of energy through the nuclear fission process. Every activity requires conventional NDT techniques to be conducted to maintain the safe working and operation of the plants and facilities. The standard NDT methods applied to *e.g.* inspection of welds in piping, are (Willcox and Downes, n.d.):

- Radiography testing (RT)
- Magnetic particle crack detection (MT)
- Dye penetrant testing (PT)
- Ultrasonic flaw detection (UT)
- Eddy current and electromagnetic testing (ET).

This paper does not focus on the so-called conventional NDT techniques and their application in the nuclear sector, but rather on the non-conventional NDT techniques that are used as needed, and which constitute important research tools. In particular, penetrating radiation probes as realized in radiography/tomography are described with specific applications in material research. Quantitative and/or qualitative data obtained through applying these novel techniques in a laboratory environment adds value to many areas within the nuclear sector. The following specific activities, ranging from mining the ore to security of the waste generated, and where radiography and tomography are applied, are highlighted in this paper:

- Mining and geosciences: quantification of ore deposits
- Fuel fabrication: development and testing of new materials
- Electricity generation: fuel rod performance ; post-irradiation examination (PIE)
- Radioactive waste: safe storage, civil engineering.

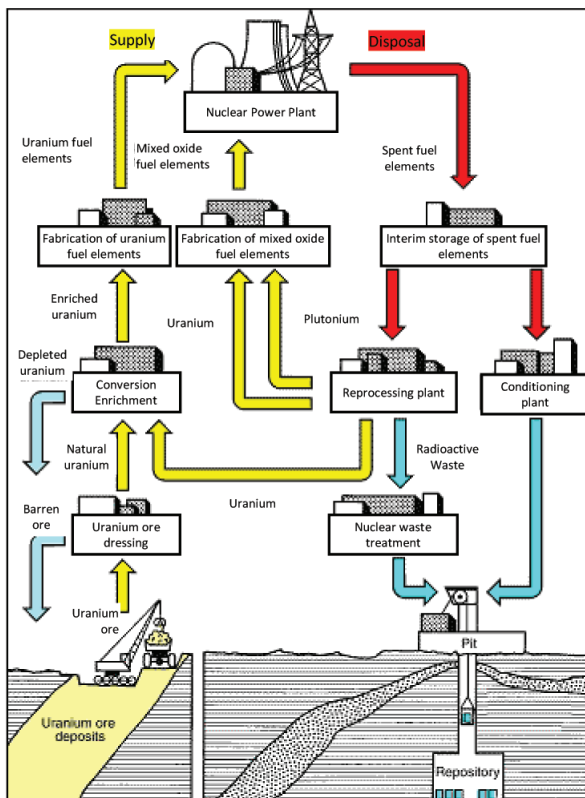


Figure 1 – Schematic depiction of the nuclear fuel cycle (Pixshark, n.d.)

### Analytical methods based on penetrating radiation

Information about the internal structures of objects, for example the hydrogen content of Zr cladding, can be obtained by destructive analytical methods, *e.g.* cutting a the fuel rod in a 2D plane for analysis by electron microscopy, or sieve analysis for particle size distribution of a soil sample. In most cases, once the sample has been destroyed, no other analytical tests are possible and the larger picture (volumetric hydrogen distribution and particle size distribution in the soil) is lost.

More valuable, unique, and in some cases more accurate results can be obtained only when three-dimensional information is available. For research purposes the most acceptable way to obtain information while maintaining the sample integrity is to apply a non-destructive test using penetrating radiation (either with X-rays, gamma rays, or neutrons). It is worthwhile to mention that the neutron, the fission product of the nuclear fuel cycle, can be used as a probe to investigate the integrity of the nuclear fuel itself. After irradiation the physical condition of fuel pellets, while still intact in the fuel pin, can be obtained only by means of radiography. This manner of non-invasive investigation keeps the sample intact, leaves the sample in its original form, and it is possible for other tests to be conducted subsequently on the real sample as if it was not touched. The non-invasive process allows for the generation of valuable qualitative information. However, when digital data is transformed into three-dimensional tomographic data (Banhard, 2008), it is possible to obtain high-resolution quantitative information of the internal structures and properties of the object. An example is the volumetric pore size distribution of voids within nuclear-encapsulating concrete matrixes, as well as their physical distribution throughout the sample (McGlenn *et al.*, 2010).

X-ray, gamma-ray, and neutron radiation are attenuated (absorbed and scattered by the sample) according to an exponential law (De Beer, Middleton, and Hilson, 2004):

$$I(E) = I_0(E)e^{\mu(E)\rho x} \quad [1]$$

where  $I$  is the intensity of the transmitted radiation beam,  $I_0$  the intensity of the incident radiation beam,  $\mu$  the attenuation coefficient ( $\text{cm}^2/\text{g}$ ) of the material under investigation for the specific radiation type,  $\rho$  the density of the sample ( $\text{g}/\text{cm}^3$ ), and  $x$  the thickness of the sample ( $\text{cm}$ ).

The attenuation coefficient  $\mu$  expresses the total attenuation, due to both the scattering and capture processes for the incident radiation. The term  $\mu\rho$  is also called the total absorption coefficient of the sample. We assume that the quantity  $\mu\rho$  is linearly related to its constituents:

$$\mu\rho = \sum (\mu_i)(\rho_i)(V_i) \quad [2]$$

where  $\mu_i$  is the radiation attenuation coefficient of constituent  $i$ ,  $\rho_i$  the density of constituent  $i$ ,  $V_i$  the volume fraction of constituent  $i$ , and  $\sum$  the summation symbol for the  $i^{\text{th}}$  components. Composites of materials will thus have a different radiation attenuation property from the individual elements.

The parameters  $I(E)$ ,  $I_0(E)$ , and  $\mu(E)$  reflect radiation energy dependency. This dependency, in a radiography

## Neutron- and X-ray radiography/tomography

context, means that materials will attenuate different radiation types by different magnitudes and thus will yield different radiological images, and also that an element has different attenuation properties at different energy levels for the same radiation type. This implies that an element can be transparent to fast neutrons (MeV energies) but can be detected easily using thermal neutrons (eV energies). An example is the thermal neutron scattering and absorption of hydrogen and boron (Domanus, 1992).

Although the basic interaction of X-rays and neutrons with the elements differs, the principle of conducting radiography to obtain a two-dimensional radiograph/image of the sample is the same. Figure 2 schematically illustrates the basic components and layout of a radiography facility.

A source of radiation emits penetrating radiation towards a sample. For example, a sample contains either a defect, an inclusion of another material, or a void that is abnormal for the sample, or an area that differs completely in terms of composition from the basic matrix of the sample, which results in a lower or higher density at the location within the sample. The incident radiation will be attenuated (scattered and/or absorbed) differently due to the abnormality. A sensitive area detector, with a high quantum efficiency for the detection of the specific type of penetrating radiation, registers the difference in attenuated radiation that has passed through the sample. The 2D data (image) obtained by

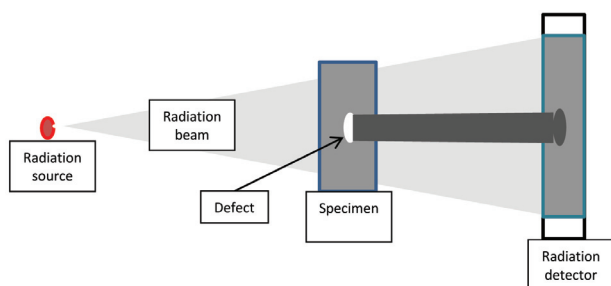


Figure 2 – Principle and layout of a 2D radiography set-up. A similar set-up is used for tomography, with the sample rotating in the radiation beam (Domanus, 1992)

the detector is called a radiograph and contains the integrated radiation transmitted information for the total sample in a certain orientation with respect to the source and detector configuration.

The information captured in the radiograph differs in principle for X-ray and neutron radiography/tomography. The two probes are mostly utilized within the nuclear fuel cycle as non-destructive techniques in research and for nuclear material qualification and quantification. These principles are discussed in more detail in the following paragraphs.

### X-ray radiography

X-ray interaction with materials depends on the density of the sample – *i.e.* the electron cloud density (Banhard, 2008). The area detector registers a two-dimensional image (radiograph) of the object representing the internal structure density. Elements with low electron densities are not easy to resolve in a radiograph, but they are easily penetrated to reveal denser materials embedded within the sample matrix. Figure 3 presents the different X-ray attenuation coefficients ( $\text{cm}^{-1}$ ) for 125 kV X-rays for the full spectrum of elements in the periodic table. It clearly shows the increase in absorption of X-rays (darker shading) at higher atomic numbers.

### Neutron radiography

The interaction of neutrons with materials is totally different to that of X-rays, since neutrons, being neutral particles, interact only with the nucleus of the atom. Neutrons are not affected by even a dense electron cloud, *e.g.* of a lead atom ( $\mu_{\text{pn}} = 0.38 \text{ cm}^{-1}$ ). The thermal neutron attenuation coefficients depicted in Figure 4 shows a totally different, and in some instances an opposite attenuation capability (grey scale) to that for X-rays (Figure 3). Hydrogen, as a highly attenuating material ( $\mu_{\text{pn}} = 3.44 \text{ cm}^{-1}$ ), will be easy to detect and clearly visible on a neutron radiograph when embedded in *e.g.* a  $\text{Zr}^{\text{TM}}$  ( $\mu_{\text{pn}} = 0.29 \text{ cm}^{-1}$ ) fuel pin, which is nearly transparent to neutrons. A radiograph with low- to intermediate-energy X-rays is possible as the  $\text{Zr}^{\text{TM}}$  tube ( $\mu_{\text{px}} = 2.47 \text{ cm}^{-1}$ ) attenuates most of the X-ray radiation and with no photons remaining, the H ( $\mu_{\text{px}} = 0.02 \text{ cm}^{-1}$ ) cannot be registered/detected on the X-ray radiograph.

Attenuation coefficients for 125kV X-Rays ( $\text{cm}^{-1}$ )																		
1a	2a	3b	4b	5b	6b	7b	8	1b	2b	3a	4a	5a	6a	7a	0			
H 0.02															He 0.02			
Li 0.06	Be 0.22									B 0.28	C 0.27	N 0.11	O 0.16	F 0.14	Ne 0.17			
Na 0.13	Mg 0.24									Al 0.38	Si 0.33	P 0.25	S 0.30	Cl 0.23	Ar 0.20			
K 0.14	Ca 0.26	Sc 0.48	Ti 0.73	V 1.04	Cr 1.29	Mn 1.32	Fe 1.57	Co 1.78	Ni 1.96	Cu 1.97	Zn 1.64	Ga 1.42	Ge 1.33	As 1.50	Se 1.23	Br 0.90	Kr 0.73	
Rb 0.47	Sr 0.86	Y 1.61	Zr 2.47	Nb 3.43	Mo 4.29	Tc 5.06	Ru 5.71	Rh 6.08	Pd 6.13	Ag 5.67	Cd 4.84	In 4.31	Sn 3.98	Sb 4.28	Te 4.06	I 3.45	Xe 2.53	
Cs 1.42	Ba 2.73	La 5.04	Hf 19.70	Ta 25.47	W 30.49	Re 34.47	Os 37.92	Ir 39.01	Pt 38.61	Au 35.94	Hg 25.88	Tl 23.23	Pb 22.81	Bi 20.28	Po 20.22	At 9.77	Rn 9.77	
Fr	Ra 11.80	Ac 24.47	Rf	Ha														
Lanthanides		Ce 5.79	Pr 6.23	Nd 6.46	Pm 7.33	Sm 7.68	Eu 5.66	Gd 8.69	Tb 9.46	Dy 10.17	Ho 10.91	Er 11.70	Tm 12.49	Yb 9.32	Lu 14.07			
Actinides		Th 28.95	Pa 39.65	U 49.08	Np	Pu	Am	Cm	Bk	Vf	Es	Fm	Md	No	Lr x-ray			

Figure 3 – Periodic table with X-ray attenuation coefficients of the elements for 125 kV X-ray energies (Grünauer, 2005)



## Neutron- and X-ray radiography/tomography

Attenuation coefficients for Thermal Neutrons (cm <sup>-1</sup> )															
1a	2a	3b	4b	5b	6b	7b	8	1b	2b	3a	4a	5a	6a	7a	0
H															He
3.44															0.02
Li	Be									B	C	N	O	F	Ne
3.30	0.79									101.60	0.56	0.43	0.17	0.20	0.10
Na	Mg									Al	Si	P	S	Cl	Ar
0.09	0.15									0.10	0.11	0.12	0.06	1.33	0.03
K	Ca	Sc	Ti	V	Cr	Mn	Fe	Co	Ni	Cu	Zn	Ga	Ge	As	Se
0.06	0.08	2.00	0.60	0.72	0.54	1.21	1.19	3.92	2.05	1.07	0.35	0.49	0.47	0.67	0.73
Rb	Sr	Y	Zr	Nb	Mo	Tc	Ru	Rh	Pd	Ag	Cd	In	Sn	Sb	Te
0.08	0.14	0.27	0.29	0.40	0.52	1.76	0.58	10.88	0.78	4.04	115.11	7.58	0.21	0.30	0.25
Cs	Ba	La	Hf	Ta	W	Re	Os	Ir	Pt	Au	Hg	Tl	Pb	Bi	Po
0.29	0.07	0.52	4.99	1.49	1.47	6.85	2.24	30.46	1.46	6.23	16.21	0.47	0.38	0.27	At
Fr	Ra	Ac	Rf	Ha											Rn
0.34															
	Ce	Pr	Nd	Pm	Sm	Eu	Gd	Tb	Dy	Ho	Er	Tm	Yb	Lu	
	0.14	0.41	1.87	5.72	171.47	94.58	1479.04	0.93	32.42	2.25	5.48	3.53	1.40	2.75	
	Th	Pa	U	Np	Pu	Am	Cm	Bk	Cf	Es	Fm	Md	No	Lr	
	0.59	8.46	0.82	9.80	50.20	2.86								neut.	

Figure 4 – Periodic table with thermal neutron energy attenuation coefficients of the elements (Grünauer, 2005)

### Tomography

The word 'tomography' comes from the Greek words 'to cut or section' (*tomos*) and 'to write' (*graphein*) (Banhard, 2008). Tomography is also known as computer tomography (CT) or computer assisted tomography (CAT) as in diagnostic investigations in the medical field. For the purpose of this article, the following semantics are adopted: CT in general description, XCT for X-ray computer tomography, and NT for neutron tomography. CT is a radiographic inspection method that uses a computer to reconstruct an image of a cross-sectional plane (slice) through an object (ISO 15708-1). The resulting cross-sectional image is a quantitative map of the linear radiation attenuation coefficient,  $\mu$ , at each point in the plane. The linear attenuation coefficient characterizes the local instantaneous rate at which the incident radiation is attenuated during the scan, by scatter or absorption, as it propagates through the object.

To obtain this 'map', the sample is radiographed and thus projection data is gathered from multiple directions through many angles of the sample. For the purpose of this article, no detailed description of the 3D reconstruction process of the sample is presented. To put it simply, multiple 2D-projections are fed into a dedicated computer with a specialized computer algorithm to create cross-sectional planes of the sample. When these cross-sectional planes are stacked together, a full virtual three-dimensional image (tomogram) of the sample can be viewed and analysed.

### Application of radiography and tomography within the nuclear fuel cycle

In each of the following sectors of the nuclear fuel cycle, radiography and/or tomography have been applied using either X-rays or neutrons. In some areas the application was pioneered in the early second half of the 20th century by means of film techniques. The techniques applied and the description thereof is not within the scope of this article. However, the outcomes of these film-based investigations and the results obtained will be described, together with the recent digital methods in this field.

### Mining

X-ray-, gamma-ray, and neutron tomography have demonstrated their potential in the earth sciences as important diagnostic tools to generate volumetric data on geological compositions, especially advances in the area borehole core investigations, as depicted in Figure 5. This aspect is being explored further with optimum resolution obtained through the application of micro-focus X-ray tomography, as CT complements conventional destructive analytical thin-sectioning of drill core samples (De Beer and Ameglio, 2011).

The raw material for nuclear fuel is uranium, which is a relatively common element that can be found throughout the world. Uranium is present in most rocks and soils, in many rivers, and in seawater. Uranium is about 500 times more abundant than gold and about as common as tin.

The largest producers of uranium are currently Australia, Canada, and Kazakhstan, with Namibia rated 5th and South Africa 11th globally (World Nuclear Association, 2015). The



Figure 5 – Left: the grouped pyroxene mineral (coloured red) can be clearly seen in norite (top), and different concentration of feldspar are observed in anorthosite (bottom) in a thin slice. Right: transparent corresponding neutron tomograms. The minerals shown are only pyroxenes that are present in both norite and anorthosite but at different concentrations [archives from Necsa's Nrad and MIXRAD system]

## Neutron- and X-ray radiography/tomography

concentration of uranium in the ore can range from 0.03 to 20%. Conventional mining is by open cut or underground methods. Uranium ore can be produced from a mine specifically for uranium, or as a by-product from mines with a different main product such as copper, phosphate, or gold (International Atomic Energy Agency, n.d.).

Using micro-focus X-ray CT with 100 kV potential to distinguish between gold ( $\mu\rho_X = 358 \text{ cm}^{-1}$ ) and uraninite ( $\mu\rho_X = 283 \text{ cm}^{-1}$ ), both the minerals are easy to distinguish from the matrix minerals such as pyrite ( $\mu\rho_X = 18.4 \text{ cm}^{-1}$ ), zircon ( $\mu\rho_X = 45.9 \text{ cm}^{-1}$ ), and brannerite ( $\mu\rho_X = 89.6 \text{ cm}^{-1}$ ) due to their much higher elemental densities. The use of CT as a sorting method is still a challenge, as it is difficult, at the 100 kV X-ray energy CT capability available, to distinguish between gold and uraninite (Chetty *et al.*, 2011). In a follow-up 3D micro-focus X-ray computer tomography ( $\mu$ XCT) study using 120 kV, the contrast and resolution of the minerals were well defined and individual minerals could be separated and distinguished from other minerals (Sebola, 2014). For the detection of uranium, 3D-CT was benchmarked against 2D mineralogical results from optical microscopy and scanning electron microscopy (SEM). Uraninite, brannerite, and uraniferous leucoxene are the uranium-bearing minerals present in the samples (from the Vaal Reef) and were quantified by  $\mu$ XCT-3D analysis for their sizes, shapes, and distribution with respect to other mineral components in the samples. Uraninite was found to be the major mineral, occurring mainly in the quartz matrices and also associated with carbonaceous matter as depicted in Figure 6. The uraninite and gold in the matrix occurred as rounded grains up to 200  $\mu\text{m}$  in size, as observed by 2D mineralogical techniques. CT allows for 3D grain size analyses of the uraninite grains in the total volume of the sample, and in this study also their association with matrix minerals, as depicted in Figure 7. The CT observations supported the results acquired by conventional mineralogical techniques, suggesting that 3D  $\mu$ XCT can be used to complement other mineralogical techniques in obtaining 3D information. However, 3D  $\mu$ XCT has limitations such as spatial resolution, partial volume effect, and overlapping of mineral grey-scale values. It is therefore suggested that the

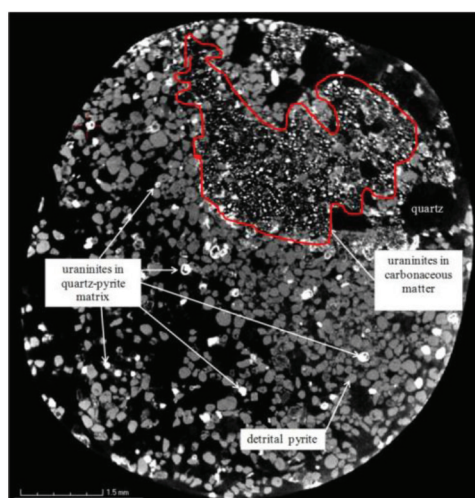


Figure 6 – X-ray CT-tomogram slice showing the distribution of uraninite grains in the quartz-pyrite matrix and the carbonaceous matter (Sebola, 2014)

technique cannot be used as an independent tool for mineral characterization, but rather in support of existing mineralogical techniques. However, valuable information is added into the nuclear value chain via 3D-CT. No sample preparation is needed other than cutting a small piece of rock for analysis. The sample integrity is maintained due to the non-destructive nature of the technique, as it provides 3D information for the total volume of the sample, including internal components. Results can be obtained within about 1 hour scan at high resolution with up to 2000 projections, providing resolution down to 6  $\mu\text{m}$  (including reconstruction).

### Enrichment

Enriched uranium is uranium in which the concentration of U-235 has been increased through the process of isotope separation. U-235 is the only nuclide existing in nature (in any appreciable amount) that is fissile with thermal neutrons (OECD Nuclear Energy Agency, 2003). Natural uranium is 99.284% U-238 isotope, with the U-235 isotope constituting only about 0.711%.

The very first application of neutron radiography was in the early 1960s for nuclear fuel characterization using the film technique. The use of neutron radiography in the monitoring of isotopic enrichment in fuel pellets loaded into a fuel pin has been demonstrated by Frajtag (n.d.) (Figure 8).

Gosh, Panakkal, and Roy (1983) investigated the possibility of monitoring plutonium enrichment in mixed-oxide fuel pellets inside fuel pins using neutron radiography as early as 1983. Recently, Tremsin *et al.*, (2013) investigated the very large difference in the absorption cross-sections of U-235 and U-238 isotopes, as shown in Figure 9, and deduced that very accurate non-destructive spatial mapping of the enrichment level of fuel pellets, as well as of the distribution of other isotopes in the spent fuel elements (Nd, Gd, Pu, *etc.*), can be achieved.

Additionally, information on the distribution of isotopes can then be used for the investigation of fuel burn-up rates for fuel elements placed at different rod positions in the reactor core.

Large differences in transmission spectra allow very accurate mapping of isotopic distributions in the samples using either transmission radiography or neutron resonance absorption characteristics of the respective isotopes (Tremsin *et al.*, 2013). One of the attractive features of energy-

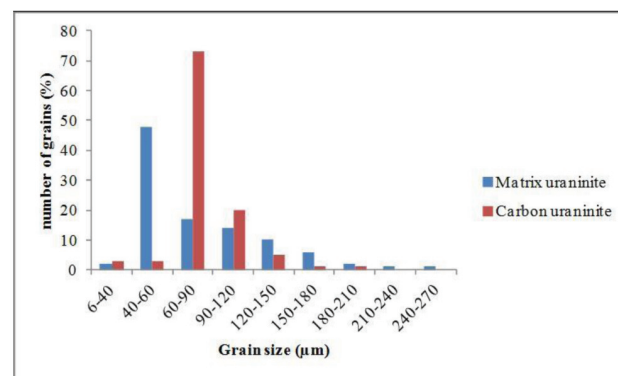


Figure 7 – Grain size distribution of uraninite in the matrix and the carbonaceous matter (Sebola, 2014)

## Neutron- and X-ray radiography/tomography



Figure 8 – Neutron radiograph (film) of fresh fuel pellets in a fuel pin with varying degrees of isotopic U-235 enrichment. Pellets with higher enrichment appear darker (Frajtag, n.d.)

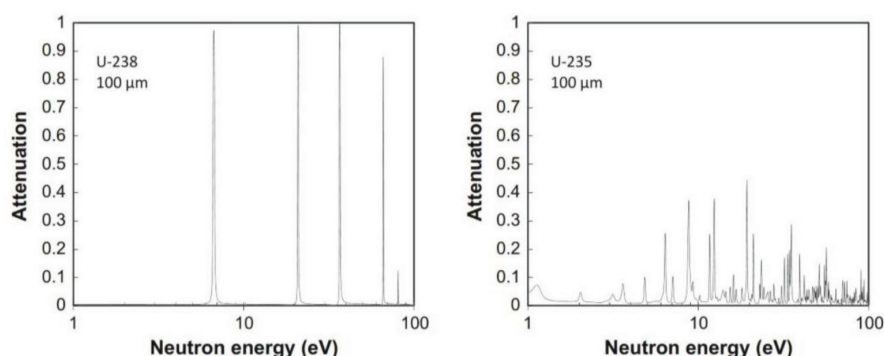


Figure 9 – Neutron attenuation of 100  $\mu\text{m}$  thick U-235 and U-238 isotopes calculated from the tabulated data on the total cross-sections as a function of neutron energy (Tremisn *et al.*, 2013)

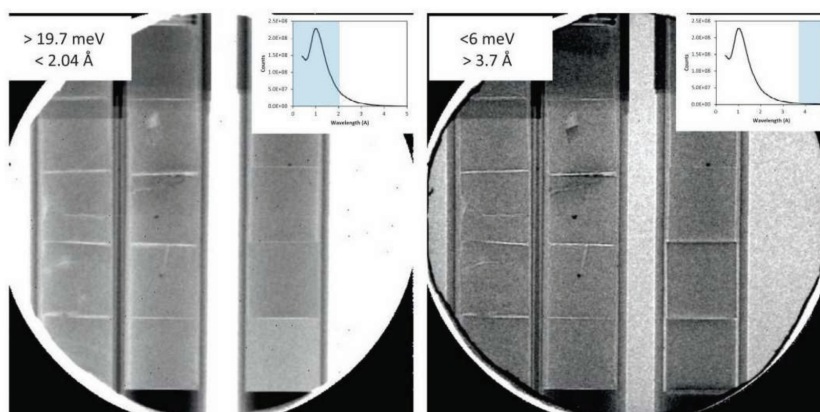


Figure 10 – Thermal neutron transmission radiographs obtained by grouping the energy-resolved images of different neutron spectra. The ranges of neutron energies used to build each radiograph are shown in the respective legends (Tremisn *et al.*, 2013)

resolved neutron radiography is the ability to enhance contrast, and in some cases enable quantification, as shown in Figure 10. It was observed that the contrast between the pellets of different density depends strongly on the range of neutron energies used. The more thermal part of the beam spectrum (neutron energies above 19.7 MeV) reveals the pellet with the lowest density as an object with the highest transmission. The coldest part of the neutron spectrum (neutron energies even below 6 MeV) shows the least dense pellet as a darkest in the assembly.

### Nuclear fuel fabrication and testing (I & PIE)

Nuclear fuel types range from isotopic sources in a form of salt or disks to pressurized water reactor (PWR) fuel in the form of  $\text{UO}_2$  fuel pellets inside  $\text{Zr}^{\text{TM}}$ -cladded fuel pins. Nuclear fuel is subjected to stringent manufacturing and

performance criteria which have to be verified. Non-destructive testing of the fuel ensures that other tests can be performed subsequently and that the material can still be applied in its specific environment. Some of the NDT tests are applied to characterize and/or quantify the integrity of the fuel or as quality assurance tests. X-ray radiography cannot be used for irradiated fuel inspection, whereas neutron radiography becomes possible due to the following reasons (Lehmann, Vontobel, and Hermann, 2003):

- Uranium has a very high attenuation coefficient for X-rays (about  $50 \text{ cm}^{-1}$  at 150 keV). The diameter of fuel pellets is in the order of 10 mm and penetration by X-rays is impossible. High-energy gamma radiation ( $>1 \text{ MeV}$ ) is, however, suitable for quality control of fresh fuel pellets
- The neutron attenuation coefficient for the natural



## Neutron- and X-ray radiography/tomography

composition of uranium is low ( $0.8 \text{ cm}^{-1}$ ) and it is easy to transmit neutrons through thicker assemblies

- U-235 and U-238 have very different interactions with thermal neutron beams. Due to the 60 times higher cross-section of U-235, it is very easy to distinguish between the two isotopes and to quantify the amount of the fissile isotope U-235
- Lead is used as shielding material around fuel samples for radiation protection purposes, and thus X-ray radiography fails in transmission experiments. Neutrons, on the other hand, penetrate lead shielding with a thickness of about 15 cm and allow neutron radiography investigations
- Additional substitutes in fuel compositions, which are in use as burnable poisons but are strong neutron absorbers (*e.g.* B, Li-6, Dy, or Gd), are easily identified with neutron methods
- After long-term exposure, hydrogen can be found in the cladding outer region of fuel rods under some circumstances. X-ray radiography fails to visualize these material modifications because of the very low contrasts obtained for elements with low atomic numbers. Neutrons, on the other hand, have a high sensitivity for hydrogen, thus allowing quantification of the hydrogen content in cladding.

### Isotopes

Characterization of isotopic sources is a demanding and difficult task due to their physical size and natural radioactivity, which makes visual inspection impossible. Hoffman (2012) investigated a small radioactive radium source using high-resolution micro-focus X-ray tomography to determine whether the sample contained a powdered form of radioactive material or whether it was solid. The source contained 20 mg of radium and was in a form of a needle with a diameter of about 1 mm and about 8 mm in length – all sealed within a glass tube. Figure 11 is an XCT tomogram of the ampoule showing its serial number clearly on the outside, while Figure 12 is a slice from the 3D tomogram revealing the position of the radioactive material inside the needle.

Valuable metrology quantitative information could be deduced from the 3D tomogram of the isotope (Table I). The most important aspect for further processing of the isotope is the quantification of the volume of radioactive salt present in the needle.

### Nuclear fuel

A major field of neutron radiography application is the inspection of nuclear fuel and control rods, reactor materials and components, and of irradiation devices for the testing of nuclear fuels and materials. The fuel rods are used under extreme conditions such as very high power density,

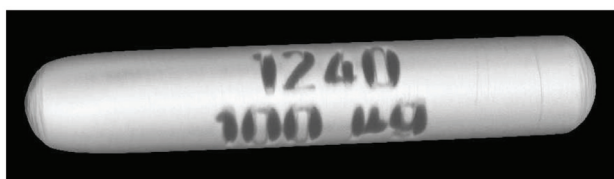


Figure 11 –  $\mu$ XCT of a Ra isotopic source ampoule (Hoffman, 2012)

Table I

#### Quantitative information deduced from the XCT

Description: Information	Value	Unit
Needle inscription	100	$\mu\text{g}$
Official source activity	20	mCi
Contact dose rate	1.1	mSv/h
Diameter of tube	1.67	mm
Diameter of internal void	1.03	mm
Length of tube	9.72	mm
Length of internal void	7.57	mm
Wall thickness	0.34	mm
Length of salt	3.01	mm
<b>Inner volume</b>	<b>6.31</b>	<b><math>\text{mm}^3</math></b>
Volume of salt	2.51	$\text{mm}^3$

temperature, pressure, and radiation level. Thermal neutron radiography investigations were conducted with the conventional film technique due to the radioactivity of the objects. The following issues are addressed through the use of neutron radiography: (a) condition of the fuel assembly, including fuel rod condition, (b) detection of leaks such as ingress of water, and (c) quality control, including functional and dimensional evaluation and inspection of irradiation devices and components. Figure 13 shows a neutron radiograph of a fuel pin with pelletized fuel as fabricated (Domanus, 1992).

Due to the high radioactivity of nuclear fuel after irradiation, X-ray radiography cannot be used as an investigation technique. Investigations are done within a hot-cell laboratory set-up, which allows for the remote handling of the radioactive fuel (Klopper, De Beer, and Van Greunen, 1998). A research reactor is normally an extension of a hot-cell laboratory, as neutron radiography is one of the major analytical probes in the post-irradiation examination (PIE) of nuclear fuel. Typical findings using neutron radiography as an analytical probe on irradiated fuel pins are the condition of the fuel pellets and of the  $\text{Zr}^{\text{TM}}$ -cladding material.

Fuel pellet investigations reveal fabricated conditions such as cracks, chips, change of shape or location, voids, inclusions, corrosion, nuclear properties, and coolant. Figure 14 shows examples of these findings on film neutron radiographs.

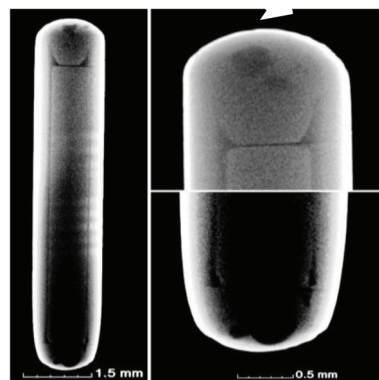


Figure 12 – Slice of  $\mu$ XCT tomogram with enlarged end pugs revealing Ra isotope internal information (Hoffman, 2012)

## Neutron- and X-ray radiography/tomography

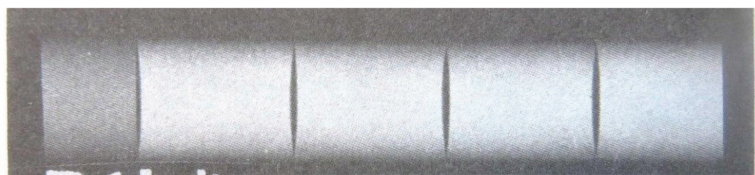


Figure 13 – Neutron radiograph of nuclear fuel prior to irradiation (Domanus, 1992)

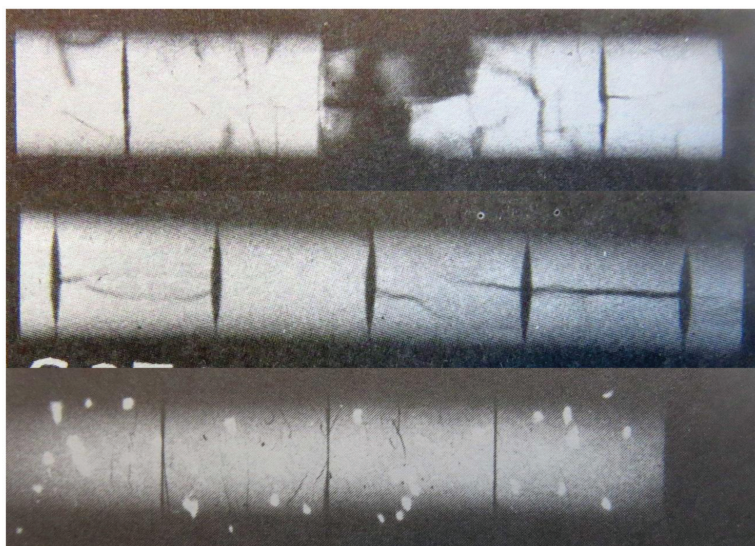


Figure 14 – Neutron radiographs (film prints) of irradiated nuclear fuel and their conditions (Domanus, 1992). Top: random cracks in pellets, middle: typical longitudinal cracks in pellets

Domanus (1992) describes a number of other fuel pellet properties revealed by neutron radiography, including central voids and the accumulation of Pu in the central void. Fuel rod inspections include deformed cladding, hydrides in cladding, plenum and spring, dislocated disks, condition of the bottom plug, and a picture of a melted thermocouple inside the fuel rod. Lehmann, Vontobel, and Hermann (2003) report on the extensive utilization of the NEUTRA and ICON neutron radiography (Nrad) facilities at Paul Scherrer Institute in Switzerland, where a dedicated detection station is available for the inspection of irradiated fuel assemblies. Aspects such as fuel enrichment, fuel poisoning, and hydrogen content in the fuel cladding are being addressed and investigated by neutron radiography. Due to the importance of fuel cladding investigations, the utilization and function of neutron radiography is addressed in the following paragraph.

### Hydrogen embrittlement

It is well known that hydrogen agglomeration is deleterious in any material. More than a few hundred ppm hydrogen in the cladding surface of fuel rods compromises the structural stability of the cladding tube significantly, with the consequence of possible failure, especially when mechanical loading is also involved. The ability of neutrons to penetrate uranium is considerably higher than for X-rays and allows for the structures of the nuclear fuel rods to be inspected. Furthermore, the probability of neutron interaction with hydrogen is very high, while for X-rays it is effectively zero. This allows neutron radiography to be effectively utilized for

the study of even small quantities of hydrogen ingress in the cladding, which is an important mechanism for cladding embrittlement, as depicted in Figure 15.

Furthermore, through proper characterization and with the aid of digital radiographs, Nrad allows for the investigation of the absolute hydrogen content and its distribution. *in situ* investigations provide new information about the kinetics of hydrogen uptake during steam oxidation and of hydrogen diffusion in zirconium alloys. Nrad-studies are the only way to investigate and understand the phenomenon of hydrogen ingress in the Zr<sup>TM</sup> cladding. A linear dependence of the total macroscopic neutron cross-section on the H/Zr<sup>TM</sup> atomic ratio, as well as on the oxygen concentration, was found, while no significant temperature dependence of the total macroscopic neutron cross-sections of hydrogen and oxygen was found, depending that zirconium and oxygen do not change their structures. Additionally, it was found that rapid hydrogen absorption takes place in the absence of the oxide layer covering the metallic surface of the Zr<sup>TM</sup> cladding (Grosse *et al.*, 2011). Figure 16 displays the results of *in-situ* Nrad investigations of hydrogen uptake during steam oxidation with the time dependence of hydrogen concentration of Zr<sup>TM</sup>-4 materials at 1273 K and higher, where a very rapid hydrogen uptake was found in the first couple of seconds after the steam flow was switched on. At temperatures of about 1273 K a phase transformation occurs and is accompanied by a volume change and the formation of a pronounced crack structure. When the cracks are formed, the



## Neutron- and X-ray radiography/tomography

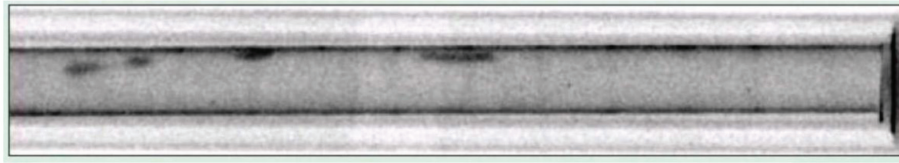


Figure 15 – Neutron radiograph of nuclear fuel and cladding material showing (black spots) hydrogen accumulation within the Zr™ tubing (Frajtag, n.d.)

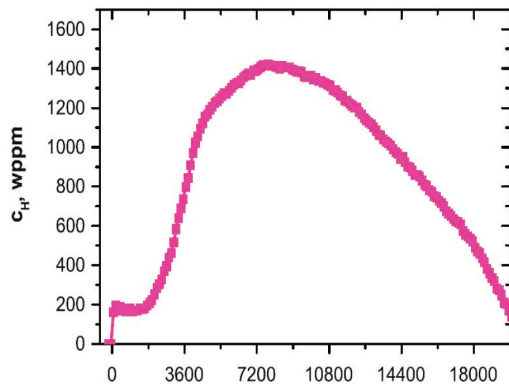


Figure 16 – Neutron radiography (Nrad) investigation: kinetics of hydrogen uptake and release during steam oxidation (Frajtag, n.d.)

hydrogen uptake increases by nearly an order of magnitude (Grosse *et al.*, 2008; Grosse, 2010). The decrease in hydrogen concentration is due to the consumption of the  $\beta$ -Zr™ phase, which contains most of the absorbed hydrogen.

### Pebble bed modular reactor (PBMR) fuel

Figure 17 shows the composition of a 60 mm outer diameter high-temperature reactor (HTR) fuel pebble consisting of thousands of 0.5 mm diameter low-enriched uranium oxide fuel particles with a tri-structural isotropic (TRISO) coating, embedded in a graphitic matrix. The pebble was analysed using X-ray tomography technique prior to irradiation at the

SANRAD facility located at the SAFARI-1 nuclear research reactor in South Africa. The aim of the investigation was to observe the homogeneity of the TRISO particles within the carbon matrix and to direct the manufacturing process to ensure the centralization of the fuel within the carbon matrix

(Necsa, 2006). Figure 18 shows the misalignment of the fuel within the carbon matrix of the fuel pebble as well as the location and identification of a TRISO particle within the fuel-free zone. The inhomogeneous distribution of the TRISO particles at the top of the fuel pebble can be clearly seen. Three-dimensional quantitative data of the misalignment of the fuel particles becomes available in the tomograms and is presented in Figure 19, showing the extent of correction in X-, Y- and Z-directions to be introduced in the manufacturing process of the fuel pebble.

Lehmann, Vontobel, and Hermann (2003) reported the successful application of neutron tomography to the 3D scanning of PBMR fuel pebbles at the NEUTRA facility of the SINQ spallation source at PSI in Switzerland (see Figure 20). A sphere-type fuel element from the high-temperature reactor (HTR) programme was studied with neutron tomography. This sample is 6 cm in diameter and contains about 8500 individual fuel pebbles (diameter 0.5 mm). No shielding of the fresh fuel element was necessary for the tomographic inspection. The investigation was aimed at the visualization of the 3D distribution of the fuel particles in the graphite matrix in order to determine its uniformity and the fuel sphere's content of fissile material.

TRISO fuel particles are an integral part of the fuel design for current and future HTRs. A TRISO particle comprises four concentric spherical layers encasing a fuel kernel, namely the buffer (porous carbon), inner pyrolytic carbon (IPyC), silicon carbide (SiC), and outer pyrolytic carbon (OPyC) layers (see Figure 17). Each layer performs specific functions. The fuel kernel, consisting of uranium or uranium carbide, provides the fissile material and retains some of the fission products. The buffer layer, a highly porous carbon structure, provides some free volume for gaseous fission products, and protects the SiC layer from damage by high-energy fission products. The IPyC layer provides structural support for the subsequent SiC layer and prevents the chlorine compounds required for SiC deposition interacting with the fuel kernel. The SiC layer forms

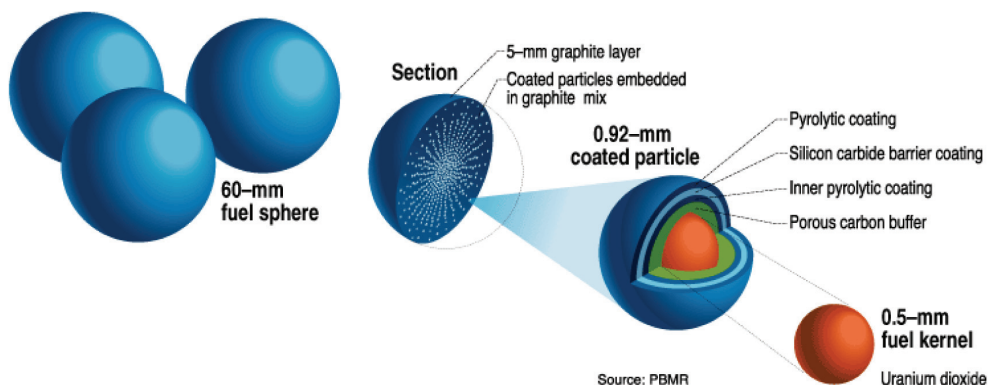


Figure 17 – Composition of PBMR fuel (Weil, 2001)

## Neutron- and X-ray radiography/tomography

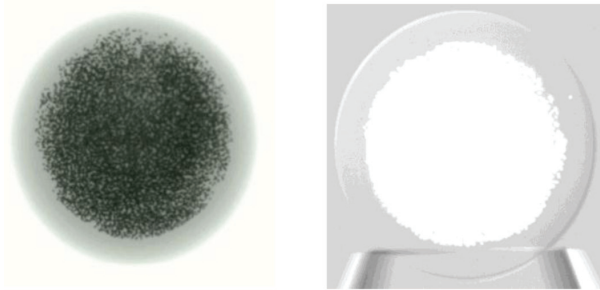


Figure 18 – X-ray tomography of a PBMR fuel pebble. Left: the non-centralized fuel sphere within the carbon matrix. Right: Location and identification of a TRISO particle inside the fuel-free zone (Necsa, 2006)

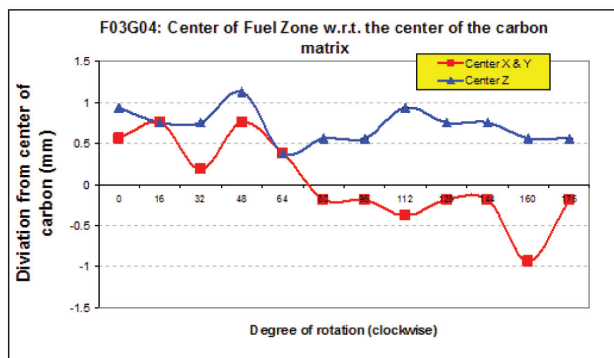


Figure 19 – Graphical presentation of the deviation of the fuel zone of a BPMP pebble from the centre of the carbon matrix in three dimensions (Necsa, 2006)

the main diffusion barrier for fission products. It acts as a pressure vessel, providing mechanical strength for the particle during manufacture of the nuclear fuel compact or pebble bed. The OPyC layer protects the SiC layer during fuel fabrication as the TRISO particle is pressed into a larger fuel compact or pebble.

Lowe *et al.*, (2015) examined the applicability of multi-scale X-ray computer tomography (CT) for the non-destructive quantification of porosity and thickness of the various layers of TRISO particles (see Figure 21) in three dimensions, and compared this to the current destructive method involving high-resolution SEM imaging of prepared cross-sections.

An understanding of the thermal performance and mechanical properties of TRISO fuel requires a detailed knowledge of pore sizes, their distribution, and interconnectivity. Pore size quantification (false color coding) and distribution in an X-ray tomogram of the SiC (D) and OPyC (E) layers within a TRISO particle is shown in Figure 22.

Direct comparison with SEM sections indicates that destructive sectioning can introduce significant levels of coarse damage, especially in the pyrolytic carbon layers. Since it is non-destructive, multi-scale time-lapse X-ray CT opens the possibility of intermittently tracking the degradation of TRISO structure under thermal cycles or radiation conditions in order to validate models of degradation such as kernel movement. X-ray CT *in situ* experimentation on TRISO particles under load and temperature could also be used to understand the internal changes that occur in the particles under accident conditions.

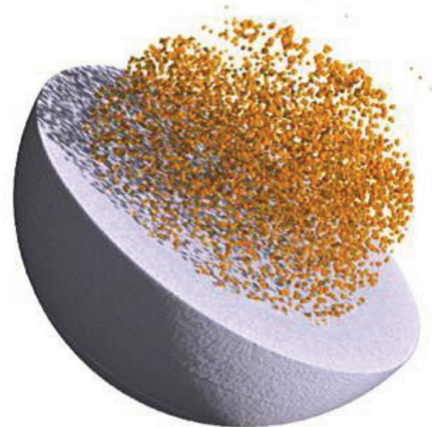


Figure 20 – Neutron tomogram generated at PSI, Switzerland showing the exact location and homogeneity of the TRISO (Lehmann, Vontobel, and Hermann, 2003)

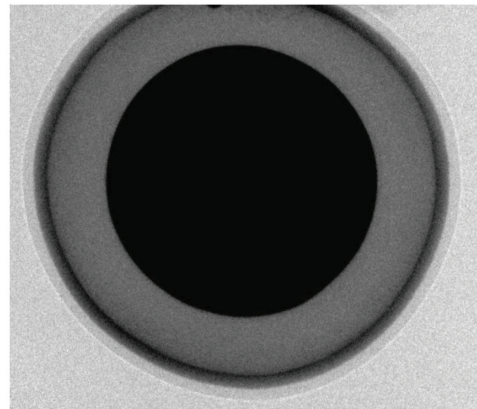


Figure 21 – Micro-focus X-ray radiograph of a TRISO particle (Necsa)

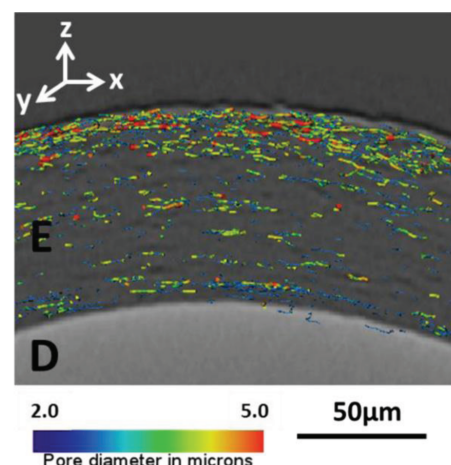


Figure 22 – Xradia VersaXRM orthoslice showing the SiC (D) and OPyC (E) layers with the pore volumes superimposed. Pore diameter is colour-coded to identify large pore clustering (Lowe *et al.*, 2015)

### Research reactor control rod verification

Nrad is being applied as a verification and analytic technique at the SAFARI-1 nuclear research reactor on the control rods

## Neutron- and X-ray radiography/tomography

prior to their installation in the core of the reactor. The quality control assurance test entails the verification of the neutron attenuation cross-section of the control rod against a standard consisting of Cd. The inspection entails a visual clarification of the attenuation of the thermal neutrons by inspection of the neutron radiograph of the control rod. Additionally, due to the digital radiography capability of the neutron camera detection system, the first-order neutron transmission calculation can be made using the pixel greyscale values on the radiographs of both the standard and control rod sample. Pixel greyscale values represent a linear relationship in the neutron attenuation of materials. In this instance a dramatic decline in greyscale pixel values is seen due to the high thermal neutron absorption by the Cd section ( $\mu_{p_n} = 115.11 \text{ cm}^{-1}$ ) of the control rod. Neutron radiographs of the Cd standard and a control rod are depicted in Figure 23.

### Radioactive waste

Low- and intermediate-level nuclear waste is normally encapsulated in in some form of barrier to protect the waste from the environment and *vice versa*. Intermediate-level nuclear waste is firstly encapsulated in a steel drum, compressed, and finally embedded normally in a concrete drum and safely stored underground in a remote location such as Vaalputs in the Karoo region in South Africa (Necsa, n.d. (b)) (see Figure 24). A site is normally chosen with low rainfall and suitable surface and groundwater conditions.

Concrete is a porous medium and the characterization of transport of water through concrete structures is well described by De Beer, Strydom and Griesel (2004) and De Beer, Le Roux and Kearsley (2005). It is especially important to understand the transport of water through concrete because nearly all concrete structures contain steel reinforcing, and in the case of nuclear waste, intermediate-level nuclear waste in compressed steel drums. When cracks in the concrete, caused by the transport of liquid through it, reach the reinforcing, an environment conducive to the corrosion of steel is created. Corrosion affects the strength of the structural members, as the steel is a major contributor to the tensile and compressive strength of the members. Severe leakage of radioactive materials into the surrounding environment is thus possible if the integrity of the concrete barrier is compromised.

Neutron radiography studies of concrete and mortars enable the direct physical visualization and quantitative detection of water inside concrete structures. The physical

properties of concrete such as porosity, permeability, and sorption characteristics are obtained through applying neutron radiography as a non-destructive analytic tool. The aim of these investigations is to maximize the properties to prevent water sorption and leaching of concrete structures and optimize one of the physical properties which is sometimes neglected in the criteria to develop structures for nuclear waste encapsulation (De Beer, Strydom and Griesel, 2004 ; De Beer, Le Roux and Kearsley, 2005). To improve the durability of concrete, the capillary and pore size within the concrete matrix must be restricted to a minimum. This is why hydration as well as W/C ratio properties is of great importance, and creates thus an ideal opportunity for neutron radiography to play a role in obtaining the needed information in a non-destructive manner to optimize these parameters. The visualization of the sorption of water by means of neutron tomography of a laboratory-size concrete structure is depicted in Figure 25.

### Conclusions

X-ray and neutron radiography in two or three dimensions play an important role in many dedicated areas within the nuclear fuel cycle. The advantage of these methods is their completely non-destructive nature. Visualization of the structure of samples, as well as quantitative description, are important aspects in materials research. The important roles of X-ray and neutron radiography/tomography as non-invasive analytic techniques within specific areas within the nuclear fuel



Figure 24 – Vaalputs intermediate-level waste storage site, South Africa (Necsa)

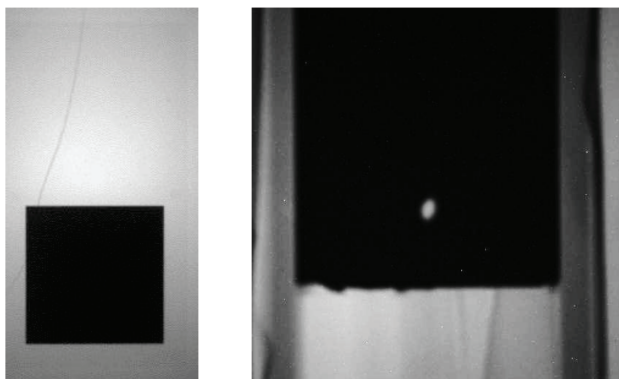


Figure 23 – Neutron radiographs of a Cd standard (left) and control rod (right) showing Cd (black) indicating high thermal neutron absorbing materials (Necsa, 2010 (a))

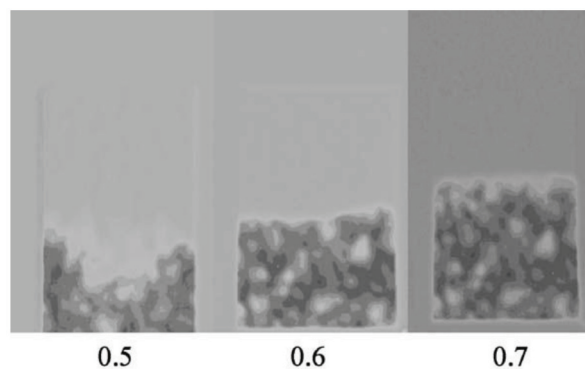


Figure 25 – Neutron radiographs showing the effect of 70%, 60%, and 50% W/C ratio on the sorptivity of water into a concrete slab (De Beer, Strydom and Griesel, 2004)



## Neutron- and X-ray radiography/tomography

cycle should not be underestimated. X-rays and neutrons are produced by very different methods, and also interact with materials in different manners. In the nuclear environment, each type of radiation has its own field of utilization due to their different characteristics, but in some instances their applications complement each other to reveal comprehensive information.

Neutron transmission analysis is a very helpful tool to obtain information on the properties of, and changes in, nuclear fuel material. Scientists and researchers in the geosciences in South Africa have, in the availability of the tomography facilities at Necsa, the capabilities to conduct quantitative analytical measurements at state-of-the-art radiation imaging facilities that compare to similar facilities elsewhere in the world.

Within the mining area, 3D computer tomography shows potential for further development, and can be already used to complement and add value to current conventional 2D mineralogical techniques. Neutron radiography analysis is able to derive the hydrogen content in fuel cladding both qualitatively and quantitatively, with high sensitivity and precision.

The results presented here illustrate how recent advances in laboratory-based X-ray CT instruments allow the examination of TRISO particles at the nano- and micro-scales in 3D. In this case study, high-resolution X-ray CT has been shown to be a viable tool for profiling the TRISO particles in two important aspects; to characterize the individual TRISO layers with variations in thickness and their subsequent interactions, thus allowing manufacturing validation as well as assisting in working towards a mechanistic understanding of fabrication and in-service issues.

The availability of these techniques in South Africa opens new possibilities for research, quantitative analysis, and non-destructive evaluation. National capacity as well as international trends shows the ability for non-destructive testing of nuclear materials utilizing penetrating X-ray- and neutron radiation in more comprehensive and unique ways than before.

## References

- AFRICAN NDT CENTRE. <http://www.andtc.com/>
- BANHARD, J. 2008. Advanced Tomographic Methods in Materials Research and Engineering. Oxford University Press.
- CHETTY, D., CLARK, W., BUSHILL, C., SEBOLA, P.T., HOFFMAN, J.W., NSHIMIRIMANA, R.B., and DE BEER, F.C. 2011. The use of 3D X-ray computed tomography for gold location in exploration drill cores. *Proceedings of the 10th International Congress for Applied Mineralogy (ICAM)*, Trondheim, Norway, 1-5 August 2011. pp.129-136. <http://www.mintek.co.za/wp-content/uploads/2011/11/ch-17.pdf>
- DAVIES, L.M. 2000. Role of NDT in condition based maintenance of nuclear power plant components. *15th World Conference on Non-Destructive Testing*, Rome, 15-21 October 2000. <http://www.ndt.net/article/wcndt00/papers/idn078/idn078.htm>
- DE BEER, F.C. and AMEGLIO, L. 2011. Neutron, X-ray and dual gamma-ray radiography and tomography of geomaterial – a South African perspective. *Leading Edge*, June 2011. Special Edition Africa.
- DE BEER, F.C., MIDDLETON, M.F., and HILSON, J. 2004. Neutron radiography of porous rocks and iron ore. *Applied Radiation and Isotopes*, vol. 61. pp. 487-495.
- DE BEER, F.C., STRYDOM, W.J., and GRIESEL, E.J. 2004. The drying process of concrete: a neutron radiography study. *Applied Radiation and Isotopes*, vol. 61, no. 4. pp. 617-623.
- DE BEER, F.C., LE ROUX, J.J., and KEARSLEY, E.P. 2005. Testing the durability of concrete with neutron radiography. *Nuclear Instruments and Methods in Physics Research A*, vol. 542. pp. 226-231.
- DOMANUS, J.C. 1992. Practical Neutron Radiography. Kluwer Academic Publishers.
- FRAJTAG, P. Not dated. Radiation Protection and Radiation Applications: Gamma and Neutron Radiography. [http://moodle.epfl.ch/pluginfile.php/1593971/mod\\_resource/content/2/RRR-EPFL-FS2014-Week14a.pdf](http://moodle.epfl.ch/pluginfile.php/1593971/mod_resource/content/2/RRR-EPFL-FS2014-Week14a.pdf) [Accessed 1 May 2015].
- GHOSH, J.K., PANAKKAL, J.P., and ROY, P.R., 1983. Monitoring plutonium enrichment in mixed-oxide fuel pellets inside sealed nuclear fuel pins by neutron radiography. *NDT International*, vol. 16, no. 5, October 1983. pp. 275-276. DOI: 10.1016/0308-9126(83)90127-X
- GROSSE, M. 2010. Neutron radiography—a powerful tool for fast, quantitative and non-destructive determination of the hydrogen concentration and distribution in zirconium alloys. *Proceedings of the 6th International ASTM Symposium on zirconium in the Nuclear Industry*, Chengdu, China, 9-13 May 2010.
- GROSSE, M., VAN DEN BERG, M., GOULET, C., LEHMANN, E., and SCHILLINGER, B. 2011. *in situ* neutron radiography investigations of hydrogen diffusion and absorption in zirconium alloys. *Nuclear Instruments and Methods in Physics Research*, vol. A651. pp. 253-257. doi: 10.1016/j.nima.2010.12.070
- GROSSE, M., STEINBRUECK, M., LEHMANN, E., and VONTOBEL, P. 2008. Kinetics of hydrogen absorption and release in zirconium alloys during steam oxidation. *Oxidation of Metals*, vol. 70, no. 3. pp. 149-162.
- GRÜNAUER, F. 2005. Design, optimization, and implementation of the new neutron radiography facility at FRM-II. Dr. Rer. Nat. dissertation, Faculty of Physics, Technischen Universität München.
- HOFFMAN, J.W. 2012. Process description for micro-focus X-ray investigation of source at MIXRAD facility. Necsa internal report, DOC NO: RS-MFX-PRO-12002.
- INTERNATIONAL ATOMIC ENERGY AGENCY. Not dated. Getting to the Core of the Nuclear Fuel Cycle. Department of Nuclear Energy, Vienna, Austria. [https://www.iaea.org/OurWork/ST/NE/NEFW/\\_nefw-documents/NuclearFuelCycle.pdf](https://www.iaea.org/OurWork/ST/NE/NEFW/_nefw-documents/NuclearFuelCycle.pdf)
- ISO 15708-1:2002(E). Non-destructive testing — Radiation methods — Computed tomography — Part 1: Principles.
- KLOPPER, W., DE BEER, F.C., and VAN GREUNEN, W.S.P. 1998. Overview of hot cell facilities in South Africa. *Proceedings of the European Working Group 'Hot Laboratories and Remote Handling'*.
- LEHMANN, E.H., VONTOBEL, P., and HERMANN, A. 2003. Non-destructive analysis of nuclear fuel by means of thermal and cold neutrons. *Nuclear Instruments and Methods in Physics Research A*, vol. 515, no. 3. pp. 745-759. doi:10.1016/j.nima.2003.07.059
- LOWE, T., BRADLEY, R.S., YUE, S., BARI, K., GELB, J., ROHBECK, N., TURNER, J., and WITHERS, P.J. 2015. Microstructural analysis of TRISO particles using multi-scale X-ray computed tomography. *Journal of Nuclear Materials*, vol. 461. pp. 29-36. <http://dx.doi.org/10.1016/j.jnucmat.2015.02.034>
- MCGINN, P.J., DE BEER, F.C., ALDRIDGE, L.P., RADEBE, M.J., NSHIMIRIMANA, R.B., BREW, D.R.M., PAYNE, T.E., and OULFSON, K.P. 2010. Appraisal of a cementitious material for waste disposal: neutron imaging studies of pore structure and sorptivity. *Cement and Concrete Research*, vol. 40. pp. 1320-1326
- NECSA. 2006. RT-TVG-06/05: Test Report: X-Ray Radiography of PBMR-Fuel Spheres with Zirconium Particles. Internal report, SAMPLE NO: DFS-T-F03G04.
- NECSA. 2010 (a). RS-TECH-REP-10004: Neutron Radiography Quality Assurance test report of neutron absorbing material in Control Rods of the SAFARI-1 Nuclear Research Reactor (Lot/Batch No: RT-LOT-10/03). Internal report.
- NECSA. Not dated (b). Vaalputs. The National Radioactive Waste Disposal Facility. <http://www.radwaste.co.za/vaalputs%20information%20pamfile.pdf> [Accessed 1 May 2015].
- OECD NUCLEAR ENERGY AGENCY. 2003. Nuclear Energy Today. OECD Publishing. p. 25.
- PIXSHARK. Not dated. <http://pixshark.com/images-of-nuclear-fuels.htm>
- SAIW (Southern African Institute of Welding). Not dated. <http://www.saiw.co.za/>
- SEBOLA, P. 2014. Characterisation of uranium-mineral-bearing samples in the Vaal Reef of the Klerksdorp Goldfield, Witwatersrand basin. MSc dissertation, Faculty of Science, University of the Witwatersrand, Johannesburg. <http://wiredspace.wits.ac.za/handle/10539/16820?show=full> <http://hdl.handle.net/10539/16820>
- SGS SOUTH AFRICA (PTY) LTD. Not dated. <http://www.sgs.co.za/en.aspx>
- TREMSIN, A.S., VOGEL, S.C., MOCKO, M., BOURKE, M.A.M., YUAN, V., NELSON, R.O., BROWN, D.W., and FELLER, B. 2013. Non-destructive studies of fuel pellets by neutron resonance absorption radiography and thermal neutron radiography. *Journal of Nuclear Materials*, vol. 440. pp. 633-646.
- WEIL, J. 2001. Pebble-bed design returns. *Nuclear Power gets a Second Look*. IEEE Spectrum Special Report. <http://spectrum.ieee.org/energy/nuclear/pebblebed-design-returns> [Accessed 20 June 2015].
- WILLCOX, M. and DOWNES, G. Not dated. A brief description of NDT techniques. Insight NDT, paper T001. <http://www.turkndt.org/sub/makale/ornek/a%20brief%20description%20of%20ndt.pdf>
- WORLD NUCLEAR ASSOCIATION. 2015. <http://www.world-nuclear.org/info/Nuclear-Fuel-Cycle/Mining-of-Uranium/World-Uranium-Mining-Production/> [Accessed 13 May 2015]. ♦